Journal of Nuclear Materials 390–391 (2009) 751–754

Contents lists available at ScienceDirect

Journal of Nuclear Materials

journal homepage: www.elsevier.com/locate/jnucmat

Cracking failure study of ITER-reference tungsten grade under single pulse thermal shock loads at elevated temperatures

T. Hirai *, G. Pintsuk, J. Linke, M. Batilliot

Forschungszentrum Julich GmbH, IFE2 Forschungszentrum Jülich GmbH, EURATOM Association, D-52425 Jülich, Germany

ARTICLE INFO

PACS:
28.52.Fa
28.52.Lf
52.40.Hf

ABSTRACT

Crack formation in an ITER-reference tungsten grade was examined under single thermal shock loading. Typically two sorts of cracks, major cracks and microcracks, were observed at the loaded surfaces. The microstructures were quantified and the formation mechanisms were discussed. The major cracks were generated due to the brittleness of the tungsten material and microcracks were formed in a process which was initiated by plastic deformation at high temperature. The plastic deformation caused also surface elevation of the loaded area. At more intense thermal shock loading conditions, the microcracks disappeared and surface modifications due to recrystallization was observed.

1. Introduction

Tungsten (W) is a candidate material at plasma facing surfaces in future fusion devices. The advantages of W are high melting temperature, high thermal conductivity, low tritium inventory and low erosion rate under plasma loading. These physical properties make W attractive to be used as plasma facing material. The main drawbacks are its poor mechanical properties. In the present design of ITER divertor vertical targets, W material is employed as the armor material at the upper part, whereas, carbon fiber composites are used at the lower part, around the strike point, where the heat flux is the highest. In the future sets of the ITER divertor, W material is being considered to be used as only the armor material for the vertical target. Besides steady-state heat loading of 5–20 MW/m^2, the armor materials at the lower part of the targets will be exposed to transient heat loads such as edge localized modes (ELMs, in the order of 1 MJ/m^2) and disruptions (several 10 MJ/m^2) [1–3]. During these events high temperature gradients and, as a consequence, high thermal stresses are generated, resulting, in dependence on the material and the applied power density, in the formation of a melt layer, recrystallization and grain growth, material erosion and crack formation. Especially the crack formation is the major concern because of its low threshold power density and the poor mechanical properties of W materials below the ductile-brittle transition temperature (DBTT). The crack formation and growth in W material under thermal loads may cause fatal destruction of the components. Therefore, it is important to assess the cracking failure mechanisms. In this paper, the cracking failure of a W grade was examined under single pulses of thermal shock loads below the melting threshold at various elevated temperatures.

2. Experimental

The ITER-reference W grades are the deformed (rolled, swaged and/or forged) ones followed by appropriate heat-treatments to obtain better mechanical properties, e.g., strength and toughness, following the sintering process [4]. The microstructure consists of anisotropically elongated grains along the deformation axis. The elongated grain orientation is strictly defined to be parallel to the heat transfer direction. By defining the grain orientation, the crack propagation is aligned along the grain orientation and cracks running parallel to the surface that enhance the risk of delamination are minimized. The crack resistance of the materials is related to mechanical properties (strength and toughness) as well as thermal properties (thermal diffusivity and thermal expansion rate), whereas the melting resistance is mainly determined by thermal properties (thermal diffusivity and melting point). Therefore, it is essential to use a specified material in a specified direction for the cracking failure examination since materials would have different mechanical properties depending on production routes.

In this experiment, a deformed W grade delivered from Plansee AG, was used for the thermal shock tests. Cylindrical shaped specimens with a diameter of 12 mm and a height of 5 mm were prepared from a 1 m long rod (∅ 12 mm, the deformation axis along the rod) [5]. The grain orientation was parallel to the heat transfer direction, which corresponds to the ITER specification.

The thermal shock experiments were performed in the electron beam facility JUDITH [3,6] in the Forschungszentrum Jülich.

* Corresponding author. Present address: ITER Organization, Cadarache Centre, 13108 St. Paul Lez Durance, France. Tel.: +33 4 42 25 65 35.
E-mail address: takeshi.hirai@iter.org (T. Hirai).

0022-3115/$ - see front matter © 2009 Published by Elsevier B.V.
doi:10.1016/j.jnucmat.2009.01.313

Electrons are generated by a tungsten cathode and accelerated to a voltage of 120 kV. Although the acceleration voltage was high, the beam penetration was limited to about 5 μm in the solid W according to a numerical simulation. The fairly homogeneous loading was realized by the electron beam scanning with a frequency of several tens kHz in *x*- and *y*-direction over a well-defined square area. The pulsed thermal shock loading was performed by the capacitor mode operation instead of the transformer mode; thus, the beam waveform appeared to be a rectangular shape. The loading area and duration were 16 mm^2 and 5 ms, respectively. The single pulse loading was applied on the as-machined surfaces. The power density that corresponds to the respective surface temperature increase ΔT [7], was varied in the range of 0.15–0.88 GW/m^2. The loads were performed on pre-heated samples at different bulk temperatures T_0, in a range of 200–800 °C. Combining ΔT and T_0, the temperature excursion during the loads were ranging between the critical temperatures of W materials, i.e., DBTT, the temperature that W deforms plastically by thermal stresses, and recrystallization temperature.

After loading, the samples were characterized by scanning electron microscopy (SEM) and laser profilometry. The cracks were quantified and discussed in terms of crack width and crack distance.

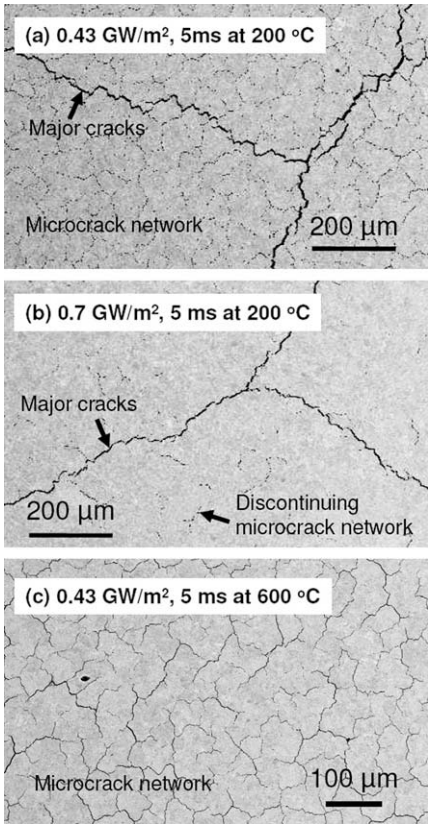

Fig. 1. Microstructures after thermal shock loads (a) 0.43 GW/m^2, 5 ms at 200 °C, (b) 0.7 GW/m^2, 5 ms at 200 °C, and (c) 0.43 GW/m^2, 5 ms at 600 °C.

3. Results and discussion

In the microstructures of the loaded samples, two sorts of cracks were found: (i) major cracks, i.e., large macroscopic cracks in the loaded area with a low crack density; (ii) microcracks, i.e., cracks appearing between major cracks and often creating a network with a comparably high crack density. Fig. 1 shows the microstructures of the loaded W samples. As shown in Fig. 1(a) and 1(b), major cracks appeared in the samples loaded at 200 °C. The major cracks were observed in all the samples loaded at 200 °C even at a power density of 0.15 GW/m^2. However, they disappeared in the samples loaded above this temperature even at highest power density. Consequently, it can be stated that the formation of the major cracks had a threshold temperature and was related to the bulk temperature T_0. This indicates that the major cracks were caused by the brittleness of the W material at this temperature, namely, below the DBTT.

As shown in Fig. 1(a) and (c), microcrack networks developed at bulk temperature ranging from 200 °C to 600 °C. The microcracks were not detected at a low power density of 0.15 GW/m^2. This indicates that the formation of microcracks had a threshold power density. Amazingly the microcrack networks started to be replaced by discontinuing networks as shown in Fig. 1(b) and disappear completely at higher power densities. No cracks were observed after loading at a bulk temperature of 800 °C; however, surface modification appeared at high power density at this temperature. Fig. 2 summarizes the microstructural observations by plotting power density (corresponding to temperature increase ΔT) as a function of bulk temperature T_0. As shown in the figure, the microcrack network was well developed at the limited power density

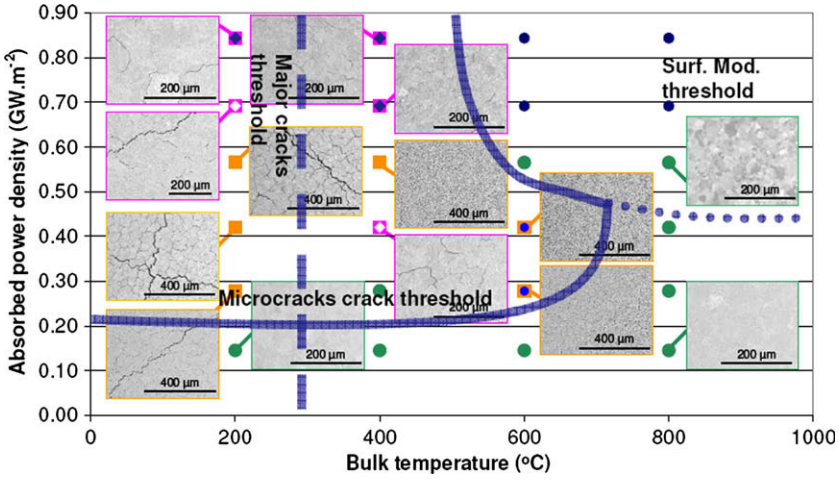

Fig. 2. Microstructures in a diagram of power density as a function of bulk temperature (T_0). The solid line indicates boundary of microcrack appearance, the dashed line for threshold of major crack generation, and the dotted line for the threshold of surface modification.

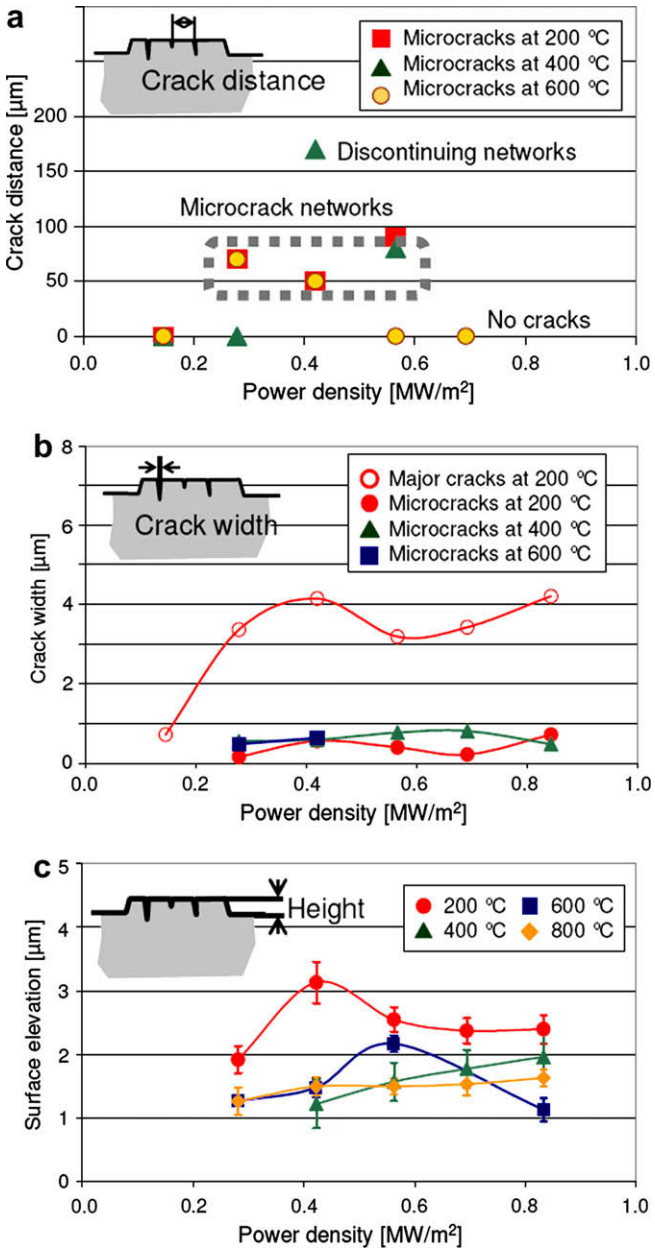

Fig. 3. Quantified data from the microstructures, (a) crack distances of microcrack networks generated from 200 °C to 600 °C (the points at *x*-axis indicate no microcracks) (b) crack width of major cracks and microcracks, and (c) height of surface elevation as a function of the power density.

range. The diagram illustrates also the safe operation conditions for the particular W grade, i.e., above 200 °C and below 0.3 GW/m^2 under these test conditions. The possible formation mechanism of the microcracks is the plastic deformation at the peak temperature. The thermal stresses (compressive stresses) induced by the high temperature gradient (expansion at the loaded surface and constraint of the cold and rigid bulk material) could exceed the yield strength of the W material at the loaded surface. Consequently, the W material deforms plastically at the peak temperature. In cooling phase the plastic strain remains in the loaded surface and tensile stresses are generated. When the tensile stresses are larger than the tensile strength of the W material, the grain boundary ruptures and opens (cracks) since grain boundaries are the weakest parts in W materials. To generate such type of cracks, the loads have to be higher than the threshold power density because the thermally induced stresses need to exceed the material strength. The disappearing of the microcracks at higher power density could be explained by the reduction of generated thermal stresses due to the decrease of the elastic modulus at the elevated temperature [4]. The modified surface microstructure at high power density loads at high temperature would be due to the recrystallization of the top surface layer. In fact, it occurred only for the loading conditions at the right top corner of the diagram i.e. power density >0.7 GW/m^2 at 800 °C (Fig. 2).

Mean crack width and mean crack distance were quantified from the microstructures. The mean crack distance, which links to the crack density, was defined by the distance between cracks. The crack distance for major cracks and discontinuing microcrack networks could not be evaluated with reasonable statistics. Therefore, only the crack distance for the network was discussed hereon. The crack distance was evaluated to be around 50–70 μm and was independent of the loading conditions. This indicated that the crack distance is determined by a constant parameter related to the W materials such as the grain size. The typical grain size of the W material is measured to be around 20 μm at the section that is slightly smaller than the observed crack distance. Most likely thermal stresses were relaxed by a plastic deformation of clusters of several grains. Fig. 3(b) displays results from mean crack width measurements. The plot shows the crack width of major cracks that appeared in samples loaded at 200 °C and microcracks that appeared from 200 °C to 600 °C. The major cracks had a maximum crack width of around 3–4 μm above 0.3 GW/m^2, whereas, the widths of microcracks were less than 1 μm and nearly independent of the loading condition. A maximum crack width of the major cracks was observed at 0.4 GW/m^2 at 200 °C (Fig. 3(b)), which is coincident with the maximum surface elevation detected by the surface profile measurement (Fig. 3(c)). Thus, the elevation is also considered to be caused by plastic deformation, i.e., volume compensation after plastic deformation at high temperature followed by crack opening during cooling. The volume compensation occurred by extending only towards the free surface since the loaded area was constrained by the surrounding rigid bulk material. The largest surface elevation, typically 2–3 μm, was observed in the samples loaded at 200 °C. The surface elevation decreased for the samples with higher base temperature T_0. Therefore, it could be concluded that the surface elevation is not due to volume expansion caused by thermal vacancy production during a quenching process which is expected to be more effective at high temperature and at high power densities.

4. Summary

By using the ITER-reference W grade, crack generation under single pulse thermal shock tests were studied in the electron beam facility JUDITH. Major cracks and microcracks appeared in the loaded area under various loading conditions. For the particular W grade, the major cracks appeared only after loading at 200 °C. This crack generation is considered to be linked to the brittleness of the W grade at this temperature. Microcrack networks developed at power densities above 0.3 GW/m^2 for pulse durations of 5 ms. The crack distance and crack width did not show a clear dependency on the loading condition. These microcracks were generated by plastic deformation at the peak temperature and by subsequent rupture at the boundary of grain clusters during cooling phase. The microcracks were found to be less developed at even more intense loading conditions. This was discussed to be due to the reduction of thermal stresses due to the decrease of elastic modulus at the elevated temperature. The height of the surface elevation of the loaded surface had maximum 2–3 μm in the samples loaded at 200 °C. The surface elevation resulted from the volume compensation after the plastic deformation.

References

[1] A. Loarte et al., Plasma Phys. Control. Fus. 45 (2003) 1549.
[2] J. Linke, T. Hirai, M. Rödig, L. Singheiser, Fus. Sci. Technol. 46 (2004) 142.
[3] T. Hirai, K. Ezato, P. Majerus, Mater. Trans. 46 (2005) 412.
[4] ITER Material Assessment Report 2001 G 74 MA 10 01-07-11 W 0.2.
[5] G. Pintsuk, W. Kühnlein, J. Linke, M. Rödig, Fus. Eng. Des. 82 (2007) 1720.
[6] R. Duwe, W. Kühnlein, H. Münstermann, in: 18th SOFT, 1994, p. 355.
[7] T. Hirai, G. Pintsuk, Fus. Eng. Des. 82 (2007) 389.